A large-scale study of the ultrawideband microwave dielectric properties of normal, benign and malignant breast tissues obtained from cancer surgeries

IOP Publishing Physics in Medicine and Biology

Phys. Med. Biol. **52** (2007) 6093–6115 doi:10.1088/0031-9155/52/20/002

A large-scale study of the ultrawideband microwave dielectric properties of normal, benign and malignant breast tissues obtained from cancer surgeries

Mariya Lazebnik[1], Dijana Popovic[2], Leah McCartney[2], Cynthia B Watkins[1], Mary J Lindstrom[3], Josephine Harter[4], Sarah Sewall[4], Travis Ogilvie[5], Anthony Magliocco[5], Tara M Breslin[6], Walley Temple[7], Daphne Mew[7], John H Booske[1], Michal Okoniewski[2] and Susan C Hagness[1]

[1] Department of Electrical and Computer Engineering, University of Wisconsin, Madison, WI, USA
[2] Department of Electrical and Computer Engineering, University of Calgary, Calgary, AB, Canada
[3] Department of Biostatistics and Medical Informatics, University of Wisconsin, Madison, WI, USA
[4] Department of Pathology, University of Wisconsin, Madison, WI, USA
[5] Department of Pathology, University of Calgary, Calgary, AB, Canada
[6] Department of Surgery, University of Wisconsin, Madison, WI, USA
[7] Department of Surgery and Oncology, University of Calgary, Calgary, AB, Canada

E-mail: mariya.lazebnik@gmail.com, hagness@engr.wisc.edu and okoniews@ucalgary.ca

Received 27 April 2007, in final form 29 August 2007
Published 1 October 2007
Online at stacks.iop.org/PMB/52/6093

Abstract

The development of microwave breast cancer detection and treatment techniques has been driven by reports of substantial contrast in the dielectric properties of malignant and normal breast tissues. However, definitive knowledge of the dielectric properties of normal and diseased breast tissues at microwave frequencies has been limited by gaps and discrepancies across previously published studies. To address these issues, we conducted a large-scale study to experimentally determine the ultrawideband microwave dielectric properties of a variety of normal, malignant and benign breast tissues, measured from 0.5 to 20 GHz using a precision open-ended coaxial probe. Previously, we reported the dielectric properties of normal breast tissue samples obtained from reduction surgeries. Here, we report the dielectric properties of normal (adipose, glandular and fibroconnective), malignant (invasive and non-invasive ductal and lobular carcinomas) and benign (fibroadenomas and cysts) breast tissue samples obtained from cancer surgeries. We fit a one-pole Cole–Cole model to the complex permittivity data set of each characterized sample. Our analyses show that the contrast in the microwave-frequency dielectric properties between malignant and normal adipose-dominated tissues in the breast is considerable, as large as 10:1, while the contrast in the microwave-frequency

dielectric properties between malignant and normal glandular/fibroconnective tissues in the breast is no more than about 10%.

(Some figures in this article are in colour only in the electronic version)

1. Introduction

According to the most recent statistics from the American Cancer Society, breast cancer is the most diagnosed cancer type among women in the United States, and ranks second among cancer deaths in women (American Cancer Society 2007). In recent years, there has been a great deal of interest in breast cancer detection and treatment techniques that utilize non-ionizing energy in the microwave frequency range (Hagness *et al* 1998, Fenn *et al* 1999, Meaney *et al* 2000, Bulyshev *et al* 2001, Fear *et al* 2002, 2003, Bond *et al* 2003, Zhang *et al* 2003, Converse *et al* 2004, El-Shenawee 2004, Huo *et al* 2004, Li *et al* 2004, Vargas *et al* 2004, Davis *et al* 2005, Fear 2005, Li *et al* 2005, Converse *et al* 2006, Kosmas *et al* 2006, Winters *et al* 2006, Xie *et al* 2006, Chen *et al* 2007, Meaney *et al* 2007, Zastrow *et al* 2007). This frequency range is particularly attractive for this application because it balances the trade-off between penetration depth and spatial resolution for imaging (detection) or focusing (treatment). The emergence of these techniques is motivated by a number of previously published studies that reported substantial contrast in the dielectric properties of normal and malignant breast tissues at radio and microwave frequencies. A summary of these studies was previously compiled in Sha *et al* (2002), and recently updated in Lazebnik *et al* (2007a).

Definitive knowledge of the dielectric properties of normal and diseased breast tissues at microwave frequencies has been limited by gaps and discrepancies associated with the above-mentioned studies. The previous studies involve small patient populations, do not include all types of normal, benign and malignant breast tissues, and, with two exceptions, do not extend above 3.2 GHz. In addition, the results of these studies are not all in agreement. To address these issues, we have conducted a large-scale study characterizing the ultrawideband dielectric properties of freshly excised breast tissues obtained from reduction and cancer surgeries, including excisional biopsies, at the University of Wisconsin (UW) and University of Calgary (UC) hospitals. The dielectric spectroscopy measurements were conducted on 488 samples from reduction surgeries and 319 samples from cancer surgeries using a precision open-ended coaxial probe in conjunction with a vector network analyzer. To the best of our knowledge, this is the most extensive microwave-frequency study to date. The results of this effort rigorously establish the microwave dielectric properties of various normal, benign and malignant human breast tissues from 0.5 to 20 GHz.

We analyzed the results of this study in two stages. In a previous paper (Lazebnik *et al* 2007a), we presented the results of the first stage of analysis, namely the characterization of the dielectric properties of all types of human *ex vivo* normal breast tissues obtained from a large number of breast reduction patients. Those results were reported separately for two reasons. First, they establish the baseline dielectric properties of normal breast tissues and degrees of normal variability. Second, they serve to validate the normal tissue data obtained from cancer specimens, where the normal samples are available near the margins of the excised specimen and are therefore generally smaller and less diverse in terms of tissue type. The results of Lazebnik *et al* (2007a) revealed two important insights: (1) the dielectric properties of normal breast tissues span a much wider range than reported in most of the previously published small-scale studies, and (2) the dielectric properties of normal breast tissues are primarily determined by the adipose content of the tissue samples. Furthermore, we found that there

was no statistically significant difference between the within-patient and between-patient variability in the measured dielectric properties.

This paper reports the results of our second stage of analysis in which we focused on the dielectric properties of normal, benign and malignant breast tissues obtained from breast cancer surgeries (lumpectomies and mastectomies) and excisional biopsies. Hereafter, both clinical procedures will be referred to as 'cancer surgeries.' We aimed to characterize the dielectric properties of a normal tissue sample and a malignant or benign tissue sample from every excised specimen. We will use the term 'sample' to refer to the region of the excised tissue specimen selected for dielectric-properties characterization.

The normal breast tissue data obtained in this second stage of our large-scale study supplement the normal breast tissue data collected and analyzed previously. Consequently, as a validation step, we first compared the dielectric properties of normal samples obtained from cancer surgeries with the dielectric properties of normal samples obtained from reduction surgeries. We subsequently compared the ultrawideband dielectric properties of normal and malignant breast tissues over the entire measurement frequency range (0.5–20 GHz). We demonstrate the critical importance of accounting for the content of adipose tissue in both normal and malignant samples in comparing their dielectric properties. Since the number of samples diagnosed as benign was substantially smaller than the number of malignant and normal diagnoses, we did not statistically analyze the differences between benign and normal, or benign and malignant breast tissues.

The remainder of this paper is organized as follows. Section 2 describes the study protocol and methods for obtaining tissue samples, acquiring and processing the data, and analyzing tissue composition. Section 3 describes the methods of statistical analysis for fitting and organizing the large data set, as well as conducting the various dielectric-properties comparisons. Section 4 discusses the results of the study, as well as a comparison between our results and those of previously published studies. The conclusions are summarized in section 5.

2. Experimental procedures

2.1. Source of tissue samples

We conducted 319 measurements on freshly excised breast tissue specimens from 196 patients undergoing lumpectomies, mastectomies, and biopsies at UW and UC hospitals. Tissues excised in the operating rooms (OR) of the respective hospitals were brought to the pathology departments where the dielectric spectroscopy characterization measurements were conducted. Measurements on normal tissue were conducted near the margins of the excised specimens, away from the site of the lesion. At both universities, the tissue handling protocols were designed to permit one measurement of diseased tissue along with one measurement of normal tissue for every excised specimen. Since the tissue handling protocols at UW and UC differed slightly, they are described separately in more detail below.

Tissue handling protocol at UC

- Tissues from all patients undergoing mastectomies and excisional biopsies at the UC hospital were made available by hospital staff through the use of the standard surgical consent form.
- Immediately following tissue excision, an OR nurse paged one of the researchers responsible for conducting the measurements (already at the hospital), who picked up the excised tissue specimen and brought it to the pathology suite. The time between excision and measurement ranged from 11 min to 4 h, with an average of about 1 h.

Figure 1. Photograph of a UW tissue specimen showing malignant tissue (white region (online), upper right) and normal adipose tissue (yellow region (online), lower left). The black ink spots mark the measurement sites. The black ink around the perimeter of the specimen denotes the margins of the excised tissue.

Tissue handling protocol at UW

- The protocol for this study was reviewed by the UW Human Subjects Committee and approved by the Institutional Review Board. Patients with intact tumors undergoing breast cancer surgeries (lumpectomies and mastectomies) at the UW hospital were identified by research nurses and approached for participation in this study. All subjects gave informed written consent prior to participation in this study.
- The excised tissue sample was transported from the OR to the pathology suite at the hospital according to standard hospital protocol. Once the excised tissue specimen was delivered to the pathology suite, the pathologist called one of the researchers (already at the hospital) to conduct the measurement. The time between excision and measurement varied from 20 min to about 4 h, with an average of about 1 h.

At each hospital, the pathologist first marked the margins of the excised tissue with ink. Subsequently, the pathologist cut a piece of tissue containing both diseased and normal tissue regions, which were immediately measured. The measurement spots were then marked with ink and the tissue was returned to the pathologist to finish processing. The photograph in figure 1 shows a representative tissue specimen obtained at UW. The black ink around the edge of the tissue specimen marks the margin of the excised tissue piece.

We recorded patient age, time between excision and measurement, and tissue temperature at the time of measurement for each sample in order to facilitate statistical analysis of the effects (if any) of these variables on the tissue dielectric properties. Tissue temperature was measured using a digital thermometer, and had often reached room temperature by the time the measurements were performed. Table 1 summarizes the details of the tissue collection and handling protocols. The range of the times between tissue excision and measurement, as well as the ranges of patient ages and tissue temperatures at the time of measurement were similar at both locations.

2.2. Microwave dielectric spectroscopy

The microwave dielectric spectroscopy technique used in this study was identical to that described in Lazebnik *et al* (2007a). Stainless steel and borosilicate glass, hermetically sealed

Table 1. Details of tissue collection and handling protocol.

Total number of patients	196
Total number of samples	319
Patient age	35–87 years (UW)
	19–90 years (UC)
Time from excision to measurement	20–221 min (UW)
	11–240 min (UC)
Tissue temperature during measurement	18.0° C–25.7° C (UW)
	19.9° C–27.2° C (UC)

flange-free precision probes were used as the dielectric sensors (Popovic *et al* 2005). The small diameter of the probe (3 mm) ensured excellent contact between the tissue and probe aperture. The hermetic seal offered protection against fluid leakage into the aperture, and ensured long-term robustness of the probe performance. The sensing depth of the probe was approximately 1–3 mm (Hagl *et al* 2003), ensuring that the probe interrogated a small tissue volume. The complex reflection coefficient at the calibration plane was recorded using a vector network analyzer (VNA) over the 0.5–20 GHz frequency range, and subsequently converted into the complex dielectric constant using the procedure described in detail in Popovic *et al* (2005). Based on characterization studies conducted previously using reference liquids, the expected uncertainty of this technique is no greater than 10% (Popovic *et al* 2005). To ensure consistent performance of this technique over time, we periodically verified its accuracy using reference liquids.

2.3. Histological analysis of tissue composition within the probe's sensing volume

As described above, the exact probe placement site was marked with ink immediately following each measurement. Histology slides were created from inked tissue sections as described in Lazebnik *et al* (2007a). Digital images of the histology slides were captured using an optical microscope, and marked with the cross-sectional dimensions of the sensing volume (3 mm × 7 mm).

The tissue composition within the sensing cross section was evaluated by a pathologist. First, the sample was diagnosed as either normal, benign or cancer. In the case of benign and cancer diagnoses, we established the type of benign tissue and grade of cancer, respectively. Second, the sample was categorized in terms of tissue composition. The tissue samples diagnosed as 'normal' were categorized in terms of percentages of adipose, glandular and fibroconnective tissues. The tissue samples diagnosed as 'benign' were categorized in terms of percentages of benign tissue. The tissue samples diagnosed as 'cancer' were categorized in terms of percentages of invasive ductal carcinoma (IDC), invasive lobular carcinoma (ILC), ductal carcinoma *in situ* (DCIS) and lobular carcinoma *in situ* (LCIS). The normal tissue that appeared on histology slides diagnosed as benign or cancer was categorized in the same way as for the 'normal' samples. In addition, the pathologist noted the percentage of necrotic tissue, if any, present in each sample. This histology analysis of the two-dimensional cross section containing the ink spot was used as an estimate of the tissue composition in the three-dimensional volume sensed by the probe. Finally, since the measured dielectric properties can be significantly influenced by the tissue type directly beneath the probe, the pathologist determined the dominant tissue type directly beneath the black ink. From this point forward, the term 'glandular' will refer to normal glandular tissue, while the term 'cancer' or 'malignant tissue' will refer to malignant glandular tissue. This is an important distinction, since the vast

majority of breast cancers arise in the glandular region of the breast, and thus breast cancer tissue is effectively malignant glandular tissue.

2.3.1. Histology-based exclusionary criteria. We applied the exclusionary criteria, reported in Lazebnik *et al* (2007a), for evaluating the quality of study-specific information preserved in the histology slides, in order to minimize uncertainty in the determination of the composition of tissue within the probe's sensing volume. The application of the criteria resulted in the exclusion of 159 samples from further analysis. Thus, 160 characterized samples remained after applying these slide-based exclusionary criteria.

3. Methods of statistical analysis

3.1. Data fitting and reduction

The data fitting and reduction techniques employed here were identical to those in Lazebnik *et al* (2007a). We fit a one-pole Cole–Cole model to each of our 160 wideband dielectric spectroscopy data sets. Cole–Cole parameter values for each complex-permittivity data set (corresponding to each characterized tissue sample) were obtained as described in Lazebnik *et al* (2007a).

3.1.1. Physics-based exclusionary criterion. A physics-based exclusionary criterion was imposed in order to ensure consistency between our data and the Kramers–Kronig relation (Lazebnik *et al* 2007a). Only five characterized tissue samples were excluded based on this criterion, leaving 155 samples from 119 patients for final analysis. The overall diagnoses of these samples were distributed as follows: 85 normal samples, 60 cancer samples and 10 benign samples.

3.2. Data analysis

3.2.1. Sources of variability. We analyzed the sources of variability in the dielectric properties at 5, 10 and 15 GHz. A nested analysis of variance (ANOVA) was used to compare patient-to-patient variability and sample-to-sample variability. Terms for diagnosis and adipose content were included in the model to ensure that these sources of variability were removed before estimating the sources of interest.

3.2.2. Effects of temperature, age and time between excision and measurement. For normal and cancer samples separately, we analyzed the effect of patient age, temperature and time from excision (the predictors) on the dielectric properties at 5, 10 and 15 GHz (the responses). We created categorical variables from these continuous predictors in order to capture all possible trends rather than just linear effects. Multivariate analysis of variance (MANOVA) (Everitt and Dunn 2000) was used to assess the effect of each predictor on the dielectric properties for each of the two diagnoses. MANOVA provides a more powerful analysis when the response has two related dimensions. It compares the 2D distribution of the responses of the groups (malignant versus normal), rather than one dimension at a time. The multivariate response was dielectric constant and effective conductivity. The MANOVA models included a term for per cent adipose and per cent fibroconnective to remove the effects of those tissues before testing for the effect of each predictor. For the predictors that showed statistical significance, we followed up the overall MANOVA F-test with pairwise analyses to assess differences between

the individual predictor categories. The same MANOVA model was used in the paired tests as in the overall test.

3.2.3. Inter-rater analysis. We conducted an inter-rater analysis to verify that the UW and UC pathologists used similar methodology to evaluate the histology slides. This verification was a critical step towards ensuring that the data collected at UW and UC could be self-consistently combined. We randomly selected ten slides (tissue samples) from each university and each pathologist analyzed the tissue composition on all 20 slides. Then, we quantitatively evaluated the agreement between pathologists using the kappa statistic. A kappa value of less than 0 indicates no agreement, while a kappa value of 1.0 indicates perfect agreement.

3.2.4. Comparison between dielectric properties of normal breast tissues obtained from reduction and cancer surgeries. To summarize the normal tissue samples from the cancer surgeries, we formed three groups of tissue samples. The three divisions were based only on the per cent adipose tissue in each sample and were chosen to maximize the difference between the groups and minimize the variability within the groups. Group 1 contained all samples with 0–30% adipose tissue (the high-water-content group), group 2 contained all samples with 31–84% adipose tissue, and group 3 contained all samples with 85–100% adipose tissue (the low-water-content group). Median dielectric constant and effective conductivity dispersion curves were obtained for each group by first calculating the fitted values for each sample in the group at 50 equally spaced frequency points. Second, the median value at each frequency point was calculated across samples within the group. Finally, the Cole–Cole model was fit to these median values. The resulting 'median curves' fit the median values very well in all cases. We also calculated the upper and lower quartiles (25th and 75th percentiles) of the fitted curves in each group at 5, 10 and 15 GHz to summarize the spread of the curves in each group. In order to ensure that no systematic bias was present in the dielectric-properties characterization of the normal tissue samples obtained from cancer surgeries, we visually compared these curves with the curves obtained in the same manner from breast reduction surgeries. Furthermore, for each of the three adipose tissue groups defined above, non-parametric Kruskal Wallis rank sum tests (Conover 2001) were performed for both the dielectric constant and effective conductivity at 5, 10 and 15 GHz to test for differences between reduction and cancer surgery, normal-tissue samples.

3.2.5. Comparison between normal and malignant tissue dielectric properties. We used MANOVA as described above to compare the dielectric properties of normal and malignant tissue at 5, 10 and 15 GHz. Three separate analyses were conducted. In all cases, we considered only those malignant samples that contained $\geqslant 30\%$ malignant tissue. The first analysis included all samples where the adipose tissue content was $\leqslant 10\%$. The second analysis was identical to the first but also included a term in the model to adjust for the per cent of fibroconnective tissue. The third did not restrict the per cent adipose tissue and did not adjust for fibroconnective tissue content.

4. Results and discussion

4.1. Histology

The kappa statistic calculated for the inter-rater analysis was 0.75, indicating substantial agreement in the methodology utilized by the pathologists at the two universities in evaluating

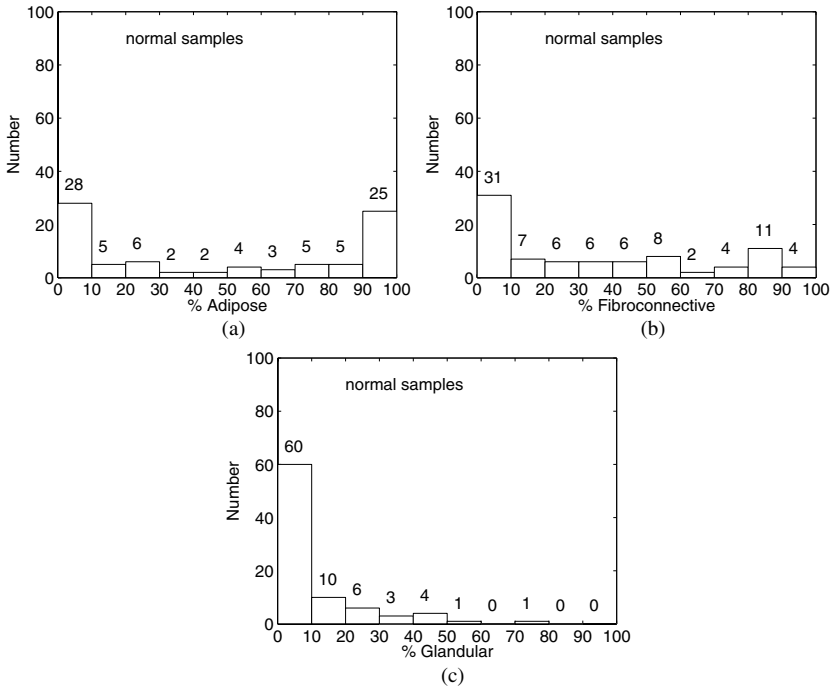

Figure 2. Histograms of the distributions of percentages of (a) adipose tissue, (b) fibroconnective tissue and (c) glandular tissue within the database of tissues with a normal diagnosis.

the histology slides. Furthermore, we found that there was no effect of location after the effects of diagnosis and adipose content were removed ($p > 0.22$). Therefore, we concluded that we could self-consistently combine the data from UW and UC into a single database.

Figure 2 shows histograms of distributions of tissues (adipose, fibroconnective and glandular) in the database of normal samples. The composition of the normal samples analyzed in this study varied greatly between low water-content and high water-content, similar to the composition of tissue samples obtained from breast-reduction surgeries. Figures 3(a)–(d) show the histograms of distributions of tissues (adipose, fibroconnective, glandular and malignant, respectively) in the database of cancer samples. Here, 'malignant' tissue refers to all cancer types found in this study (IDC, ILC, DCIS and LCIS). Furthermore, figures 3(e) and (f) show histograms of the distributions of the two dominant cancer types (IDC and DCIS, respectively) in this study. The labels 'normal samples' and 'cancer samples' in figures 2 and 3, respectively, correspond to the overall diagnosis of the tissues included in the histograms.

We note several important features of the data of figures 2 and 3. First, the adipose and glandular tissue contents of the cancer samples are very low. Specifically, 50 of the 60 cancer samples (83%) contained 0–20% adipose tissue, and all 60 cancer samples contained 10% or less glandular tissue. This is explained by the fact that the vast majority of cancer tissues analyzed in this study originated within the glandular region of the breast, so we would expect these tumors to contain very little adipose and normal (non-malignant) glandular tissues. Second, very few cancer samples contained appreciable amounts of cancer types other than IDC. This is due to the fact that IDC is the most prevalent type of breast cancer in women. The next most prevalent cancer type was DCIS: six samples contained DCIS contents of 30% or

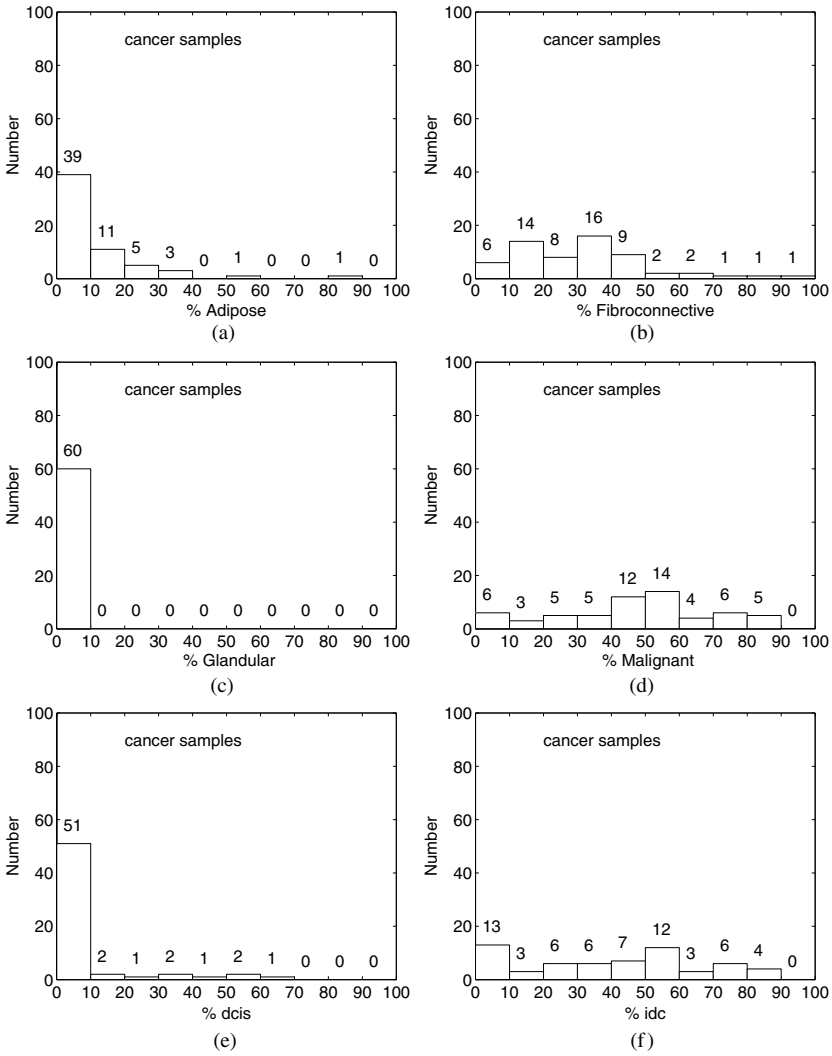

Figure 3. Histograms of the distributions of percentages of (a) adipose tissue, (b) fibroconnective tissue, (c) glandular tissue and (d) malignant tissue within the database of tissues with a cancer diagnosis. Malignant tissue includes all cancer types considered in this study: IDC, ILC, DCIS and LCIS. Histograms of the distributions of percentages of (e) DCIS and (f) IDC, the two most prominent cancer types in this study.

greater, three samples contained DCIS contents of 11–29%, and 51 samples contained 0–10% DCIS. The compositions of the other two cancer types in this study were very low: LCIS content ranged from 2 to 10% (two samples), and ILC content ranged from 1 to 10% (five samples).

4.2. Data fitting and reduction

Figure 4 shows two representative examples of the raw measurement data (circles) along with the fitted Cole–Cole curves (solid lines). Figures 4(a) and (b) show an example of a normal data set, while figures 4(c) and (d) show an example of a cancer data set. The measured

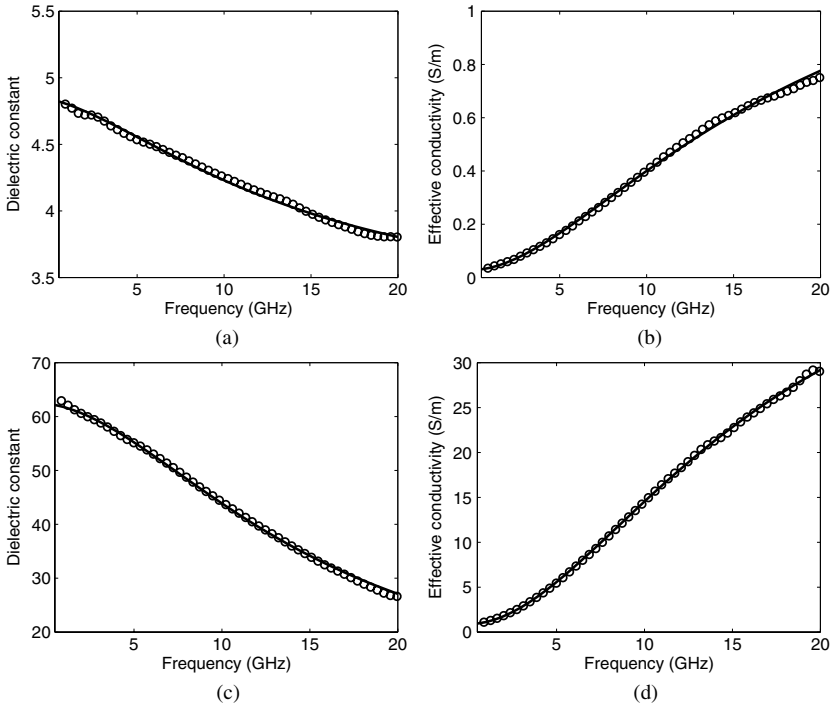

Figure 4. Examples of Cole–Cole fits to two representative experimental data sets. (a) Dielectric constant and (b) effective conductivity as a function of frequency for a normal sample; (c) dielectric constant and (d) effective conductivity as a function of frequency for a cancer tissue sample.

data were fit closely with a single-pole Cole–Cole model for both low water-content and high water-content breast tissues. We emphasize that out of 160 measurements, only five were excluded from further statistical analysis because they could not be fit with a Cole–Cole model.

Figure 5 shows the one-pole Cole–Cole curves for the 85 normal data sets, figure 6 shows the one-pole Cole–Cole curves for the 60 cancer data sets, and figures 7 and 8 show the one-pole Cole–Cole curves for the five UW benign samples and five UC benign samples, respectively. In all figures, the curves are color coded based on the adipose tissue content of each sample. In order of highest to lowest adipose content, the colors (in the online version of the journal) are red, purple, blue, cyan and green. In addition, the black curves, in order of lowest to highest dielectric properties, represent the dielectric properties of lipids (dashed lines), blood (dash-dot lines) as reported in Gabriel *et al* (1996), and 1.0 wt% saline solution (solid lines) as reported in Hilland *et al* (1997). The dielectric properties of lipids were measured in our laboratory using the same open-ended coaxial probe and technique described previously. Figures 5–8 illustrate that the dielectric properties of all tissue samples analyzed in this study are bounded from below by the dielectric properties of lipids, and from above by the dielectric properties of saline. The dielectric properties of blood are near the top of this range.

Consistent with the results of our previous analysis (Lazebnik *et al* 2007a), the dielectric properties of normal samples reported here span a very large range (figure 5). Most of the red curves (high adipose-content samples) cluster towards the low dielectric-properties end, while most of the green curves (low adipose-content samples) cluster towards the high dielectric-

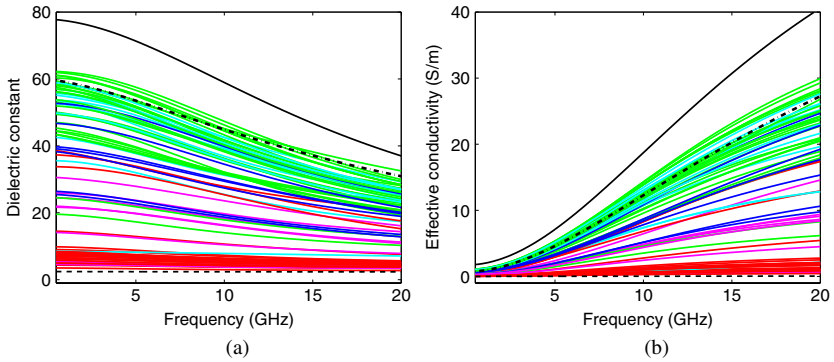

(a) (b)

Figure 5. One-pole Cole–Cole fits to the 85 normal data sets. The curves are color coded based on the amount of adipose tissue present in each sample. The solid black (upper) curve represents the dielectric properties of saline, the dashed black (lower) curve represents the dielectric properties of lipids, and the dash-dot black (middle) curve represents the dielectric properties of blood.

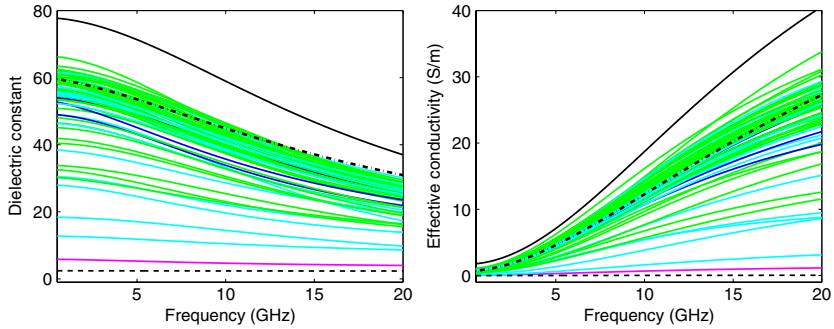

(a) (b)

Figure 6. One-pole Cole–Cole fits to the 60 cancer data sets. The curves are color coded based on the amount of adipose tissue present in each sample. The black curves are as in figure 5.

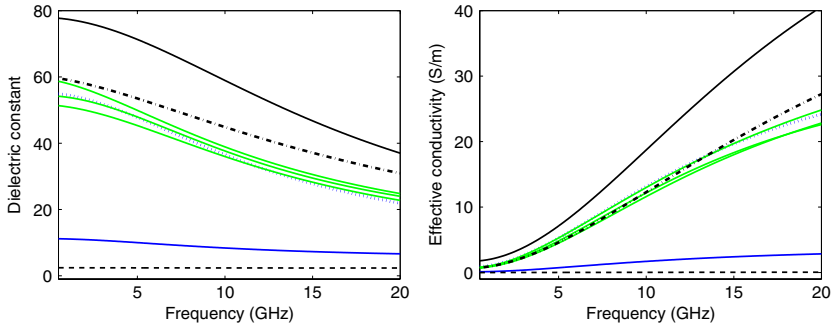

(a) (b)

Figure 7. One-pole Cole–Cole fits to the five UW benign data sets (four cystic cases, solid lines, and one ductal hyperplasia case, dotted lines). The curves are color coded based on the amount of adipose tissue present in each sample. The black curves are as in figure 5.

properties end. These observations agree with our expectations since the water content of normal breast tissues varies between very low water-content (pure adipose tissue) and very

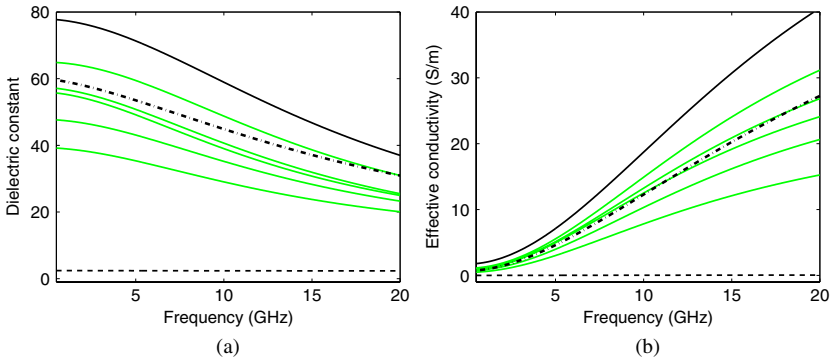

Figure 8. One-pole Cole–Cole fits to the five UC benign data sets. The curves are color coded based on the amount of adipose tissue present in each sample. The black curves are as in figure 5.

high water-content (glandular and/or fibroconnective tissues). In contrast, the majority of the Cole–Cole curves for the cancer samples are green (low adipose content), and are found towards the higher end of the dielectric-properties range (figure 6). This observation is consistent with figure 3(a), which showed that the adipose content of the majority of the cancer samples is very low.

The UW and UC benign cases were not combined into a single set because the types of benign tissues differed at the two locations: there were four cystic cases (solid lines in figure 7) and one ductal hyperplasia case (dotted lines in figure 7) at UW, while all the benign cases at UC were fibroadenomas (figure 8). The dielectric-properties dispersion curves of these generally low-adipose-content samples are found at the higher end of the range spanned by the curves for lipids and saline. We did not perform further statistical analysis on the dielectric properties of benign tissues since so few benign cases were available in this study.

4.3. Analysis of sources of variability

We found no statistically significant difference between the variability due to the patient and the variability due to the sample within the patient ($p > 0.22$). Patient-to-patient and sample-to-sample standard deviations (SDs) at 5 GHz for dielectric constant were 10.57 and 10.77, respectively. For effective conductivity, the SDs were 1.12 S m^{-1} and 1.07 S m^{-1}. Since the magnitude of these differences is very small compared to the overall large range of the dielectric-properties values, we did not include a term for the patient in further analyses.

4.4. Analysis of the effects of patient age, sample temperature and time between excision and measurement

We found that the effect of tissue temperature on the dielectric properties of the normal samples was statistically significant ($p < 0.05$). However, the temperature range of the samples characterized in this study was relatively small. Furthermore, the magnitude of the dielectric-properties changes over the small temperature range was small compared to the overall large range of the dielectric properties of normal tissue samples, and there was no identifiable pattern in the effect. Thus, we draw the same conclusion as in Lazebnik *et al* (2007a), namely that this effect does not have practical importance for engineering applications. We found no other statistically significant trends between the dielectric properties and patient age, sample temperature and time between excision and measurement for both the normal and cancer data sets.

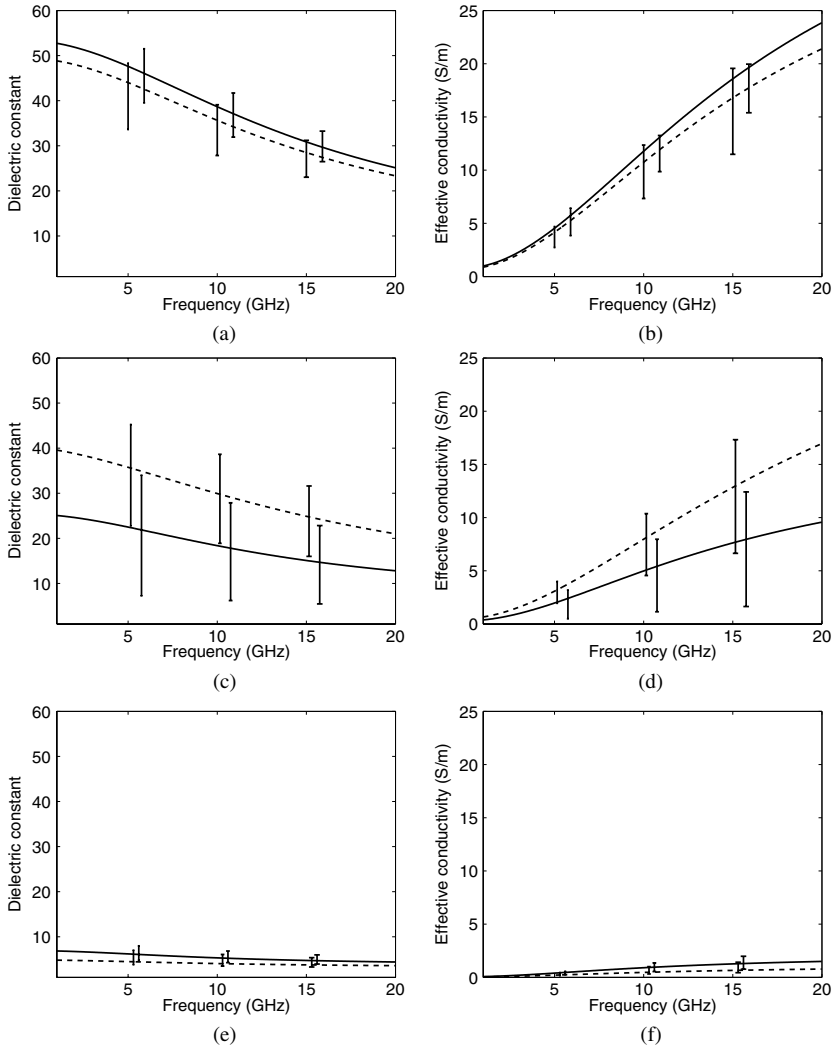

Figure 9. Median Cole–Cole curves for the dielectric properties of three adipose-defined tissue groups for the normal breast tissue samples obtained from reduction surgeries (dashed lines) and cancer surgeries (solid lines): (a) and (b) group 1 dielectric constant and effective conductivity; (c) and (d) group 2; (e) and (f) group 3.

4.5. Dielectric properties of normal breast tissue samples obtained from reduction and cancer surgeries

The normal samples obtained from cancer surgeries were distributed across the three adipose-defined tissue groups as follows: group 1 contained 39 samples, group 2 had 16 samples, and group 3 contained 30 samples. In comparison, the distribution of normal samples obtained from reduction surgeries was as follows: group 1 had 99 samples, group 2 contained 84 samples and group 3 had 171 samples (Lazebnik *et al* 2007a).

Figure 9 shows the Cole–Cole curves for the median dielectric properties of the three adipose-defined groups for breast tissues obtained from reduction surgeries (dashed lines) and

Table 2. Cole–Cole parameters for the dielectric properties of the three adipose-defined groups of normal samples obtained from reduction surgeries.

	Group 1			Group 2			Group 3		
Percentile	25th	50th	75th	25th	50th	75th	25th	50th	75th
ϵ_∞	9.941	7.821	6.151	8.718	5.573	5.157	2.908	3.140	4.031
$\Delta\epsilon$	26.60	41.48	48.26	17.51	34.57	45.81	1.200	1.708	3.654
τ (ps)	10.90	10.66	10.26	13.17	9.149	8.731	16.88	14.65	14.12
α	0.003	0.047	0.049	0.077	0.095	0.091	0.069	0.061	0.055
σ_s (S m^{-1})	0.462	0.713	0.809	0.293	0.524	0.766	0.020	0.036	0.083

Table 3. Cole–Cole parameters for the dielectric properties of the three adipose-defined groups of normal samples obtained from cancer surgeries.

	Group 1			Group 2			Group 3		
Percentile	25th	50th	75th	25th	50th	75th	25th	50th	75th
ϵ_∞	5.013	7.237	7.816	3.891	6.080	6.381	3.122	3.581	3.882
$\Delta\epsilon$	40.60	46.00	50.21	4.113	19.26	32.30	2.133	3.337	5.020
τ (ps)	10.16	10.30	10.47	13.83	11.47	10.41	14.27	15.21	12.92
α	0.091	0.049	0.055	0.038	0.057	0.081	0.099	0.052	0.059
σ_s (S m^{-1})	0.607	0.808	0.889	0.082	0.297	0.561	0.034	0.053	0.103

cancer surgeries (solid lines). The variability bars around the medians represent the 25th–75th percentiles. The Cole–Cole parameters of the curves corresponding to the 25th percentile, 50th percentile (median) and 75th percentile are shown in table 2 (reduction surgeries) and table 3 (cancer surgeries). We found statistically significant differences in the dielectric properties of normal samples obtained from reduction and cancer surgeries for all three adipose-defined tissue groups. For example, for group 1 at 5 GHz, the median dielectric constant for samples obtained from reduction surgeries was 44.2, while the median dielectric constant for normal samples obtained from cancer surgeries was 47.5. The median effective conductivities were 4.15 S m^{-1} and 4.5 S m^{-1}, for the samples obtained from reduction and cancer surgeries, respectively. For group 2 at 5 GHz, the median dielectric constants were 35.9 and 22.4, for the samples obtained from reduction and cancer surgeries, respectively. The median effective conductivities were 3.12 S m^{-1} and 1.99 S m^{-1}, respectively. Finally, for group 3 at 5 GHz, the median dielectric constants were 4.45 and 6.19, for the samples obtained from reduction and cancer surgeries, respectively. The median effective conductivities were 0.21 S m^{-1} and 0.40 S m^{-1}, respectively. The median dielectric properties at other frequencies for the three groups exhibit the same trend as at 5 GHz.

We note that the differences in the dielectric properties for groups 1 and 3 are small in light of the variability of the dielectric properties of individual curves, and thus do not signify the presence of any important bias. This is shown in figures 9(a), (b), (e) and (f), where the variability bars for the breast reduction and cancer data sets overlap. In addition, the Cole–Cole parameters for these two groups for breast tissues obtained from reduction and cancer surgeries are very similar (see Cole–Cole values corresponding to 50th percentiles in tables 2 and 3). In contrast, the differences in the dielectric properties for group 2 for breast tissues obtained from reduction and cancer surgeries are larger, which is shown in figures 9(c) and (d). The Cole–Cole curves for the median dielectric properties of group 2 for samples

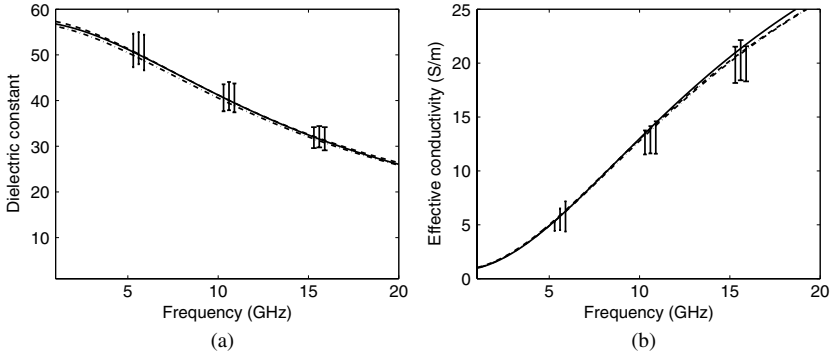

Figure 10. Median Cole–Cole curves for (a) dielectric constant and (b) effective conductivity of cancer samples with minimum malignant tissue contents of 30% (dotted lines), 50% (dash-dot lines), and 70% (solid lines). The variability bars correspond to the 25th–75th percentiles.

obtained from cancer surgeries are substantially lower than the Cole–Cole curves for the median dielectric properties of this group for samples obtained from reduction surgeries. This is also clear from the values of the Cole–Cole parameters for group 2 shown in tables 2 and 3. We attribute this observed difference to two factors. First, the number of samples contributing to the medians is very different: 84 samples for the breast reduction database, and 16 samples for the cancer database. The median estimated from a smaller number of samples is likely to be less accurate than the median estimated from a larger number of samples. Second, the distributions of tissue compositions for the samples obtained from reduction and cancer surgeries are skewed. Samples containing 51–84% adipose tissue make up three-fourths of all normal samples obtained from cancer surgeries, while they make up only half of all normal samples obtained from reduction surgeries. Since more of the samples in the intermediate group obtained from cancer surgeries have higher adipose contents than the samples obtained from reduction surgeries, it is expected that the median dielectric properties of these samples is lower. This skewed distribution of tissue compositions is a direct result of the measurement protocol employed in this study. Specifically, since we collected measurements on normal samples away from the site of the tumor, and since all of the breast tumors considered in this study arise in glandular tissues, it follows that the normal tissue samples characterized in this study had higher adipose contents than the normal tissue samples characterized in the breast reduction study.

4.6. Comparison between normal and malignant tissue dielectric properties

Figures 10(a) and (b) show the median Cole–Cole curves of cancer samples with 30% or greater malignant tissue content (dotted lines), 50% or greater malignant tissue content (dash-dot lines), and 70% or greater malignant tissue content (solid lines). Here, by 'malignant tissue content' we mean the sum of the percentages of all cancer types (IDC, DCIS, ILC and LCIS) considered in this study. The variability bars around the medians represent the 25th–75th percentiles. Restricting the minimum malignant tissue content ensured that the cancer samples included in the analysis contained sufficient malignant tissue for a meaningful analysis. The median Cole–Cole curves of samples with a higher minimum malignant tissue content (e.g. 50% or 70%) are virtually indistinguishable from the median Cole–Cole curves of samples with a minimum malignant tissue content of 30%. Furthermore, setting the minimum

Table 4. Cole–Cole parameters for the dielectric properties of 49 cancer samples that contain 30% or greater malignant tissue content.

Percentile	25th	50th	75th
ϵ_∞	7.670	6.749	9.058
$\Delta\epsilon$	43.92	50.09	51.31
τ (ps)	10.70	10.50	10.84
α	0.028	0.051	0.022
σ_s (S m^{-1})	0.748	0.794	0.899

malignant tissue content to higher values (50% or 70%) would result in less reliable results due to the smaller number of samples included in the analysis (33 or 14, respectively), compared with the 49 samples that contained 30% or more malignant tissue content. Therefore, we concluded that it was most appropriate to include all cancer samples with minimum malignant tissue content of 30% in the analyses described below. The Cole–Cole parameters of the curves corresponding to the 25th, 50th, and 75th percentiles for cancer samples containing 30% or greater malignant tissue content are shown in table 4.

We present the results comparing the dielectric properties of normal and cancer tissue samples obtained from cancer surgeries utilizing the following three techniques in our statistical analyses: (1) adjusting for adipose tissue content, (2) adjusting for adipose and fibroconnective tissue contents and (3) not adjusting for adipose or fibroconnective tissue contents.

4.6.1. Adjusting for adipose tissue content (technique 1). We found statistically significant differences between the dielectric properties of normal and cancer samples ($p < 0.07$) over the 0.5–20 GHz frequency range, when we considered only samples with maximum adipose content of 10%. Restricting the maximum adipose content to 10% allowed us to focus our analysis on high-water-content samples, without skewing the results by including normal tissues with high adipose contents. Thus, the 28 normal samples included in this analysis were composed primarily of normal glandular and/or fibroconnective tissues, while the 37 cancer samples were composed primarily of malignant glandular (IDC, DCIS), and normal fibroconnective tissues.

At 5 GHz, the mean dielectric constant for the subset of normal tissue samples described above was 46.13, while the standard error of the mean (SE) was 1.80. The mean dielectric constant for the subset of cancer tissue samples described above was 49.78 (SE = 1.17), which is 7.9% higher. Similarly, at this frequency, the mean effective conductivity for normal tissue samples was 4.39 S m^{-1} (SE = 0.18 S m^{-1}), while the mean effective conductivity for cancer tissue samples was 4.83 S m^{-1} (SE = 0.13 S m^{-1}), which is 10.0% higher. We found similar trends at other frequencies. In fact, the largest difference between the mean dielectric properties of normal and cancer breast tissue samples was approximately 11.7% (effective conductivity at 15 GHz).

It is known that malignant tumors have increased perfusion over normal tissues due to increased angiogenesis (Alberts *et al* 2002). Therefore, one might speculate that the dielectric properties of *in vivo* malignant tumors will be increased when the increased perfusion is taken into account. However, as we showed in figure 6, the dielectric-properties curves of blood are found within the cluster of curves formed by the cancer samples. Therefore, we do not expect that adjusting for the increased perfusion in malignant tissues will appreciably raise their dielectric properties.

4.6.2. Adjusting for adipose and fibroconnective tissue contents (technique 2). We found no statistically significant differences ($p > 0.12$) between the dielectric properties of normal and cancer samples when we considered only samples with maximum adipose content of 10%, and also adjusted for fibroconnective tissue content. By adjusting for fibroconnective tissue content, we are effectively conducting a direct comparison of the dielectric properties of normal glandular and malignant glandular tissues in the breast.

4.6.3. Not adjusting for adipose or fibroconnective tissue contents (technique 3). We found statistically significant differences between the dielectric properties of normal and cancer samples when we did not adjust for adipose or fibroconnective tissue contents. The malignant tissue content of cancer samples was still constrained to be $\geqslant$30%. Consequently, this analysis included 49 cancer samples and all 85 normal samples. At 5 GHz, the mean dielectric constant of normal samples was 33.84 (SE = 1.83), while the mean dielectric constant of cancer samples was 48.98 (SE = 1.09), which is 44.7% larger. The mean effective conductivity of normal samples at this frequency was 3.19 S m^{-1} (SE = 0.18 S m^{-1}), while the mean effective conductivity of cancer samples was 4.75 S m^{-1} (SE = 0.12 S m^{-1}), which is 48.9% larger. We found similar trends at other frequencies—both the mean dielectric constant and effective conductivity of the cancer samples were consistently 40–50% larger than those of the normal samples.

We emphasize that this third technique of analyzing and interpreting the data is potentially misleading if taken out of context. Since we did not adjust for adipose tissue content here, the mean dielectric properties of normal samples are strongly influenced by the dielectric properties of adipose tissue. As we showed previously in figures 2(a) and 3(a), approximately 30% of the normal samples analyzed in this study have adipose contents of 90–100%, while none of the cancer samples have adipose contents of 90–100%. Clearly, not adjusting for the content of adipose tissue between the normal and malignant samples considerably biases the results of this analysis in favor of the high adipose-content tissues, resulting in greatly reduced mean dielectric properties of the normal samples. Accordingly, this technique reveals that there is a large dielectric-properties contrast between normal *adipose-dominated* tissues and malignant glandular tissues in the breast. Referring back to figures 9 and 10, we observe a nearly 10:1 contrast between malignant tissue (figure 10) and normal tissue that is almost entirely adipose (the group 3 curves in figure 9). We reiterate that the first two techniques presented earlier in this section, which adjust for adipose and fibroconnective tissue content in the normal and malignant samples, demonstrate that there is very little contrast between normal fibroconnective/glandular breast tissues and malignant glandular breast tissues.

4.7. Variation of tissue composition with dielectric properties

Each graph in figure 11 was created by plotting three sets of data points representing tissue percentages for each sample within a specific specimen class (normal or cancer), at a position along the horizontal axis corresponding to that sample's dielectric properties at 5 GHz. Subsequently, a smoothing function was applied to the three sets of data points to create curves for each tissue type. These plots present an alternative way of viewing our data, by showing how the tissue composition of normal samples (figures 11(a) and (b)) and cancer samples (figures 11(c) and (d)) changes as the dielectric properties at 5 GHz change. Similar trends were observed at 10 and 15 GHz (data not shown). We note that figures 11(a) and (b) are very similar to figures 10(a) and (b) in Lazebnik *et al* (2007a), indicating that the tissue composition of normal samples changes in a similar way as the dielectric-properties change, regardless of whether the normal samples were obtained from reduction or cancer surgeries.

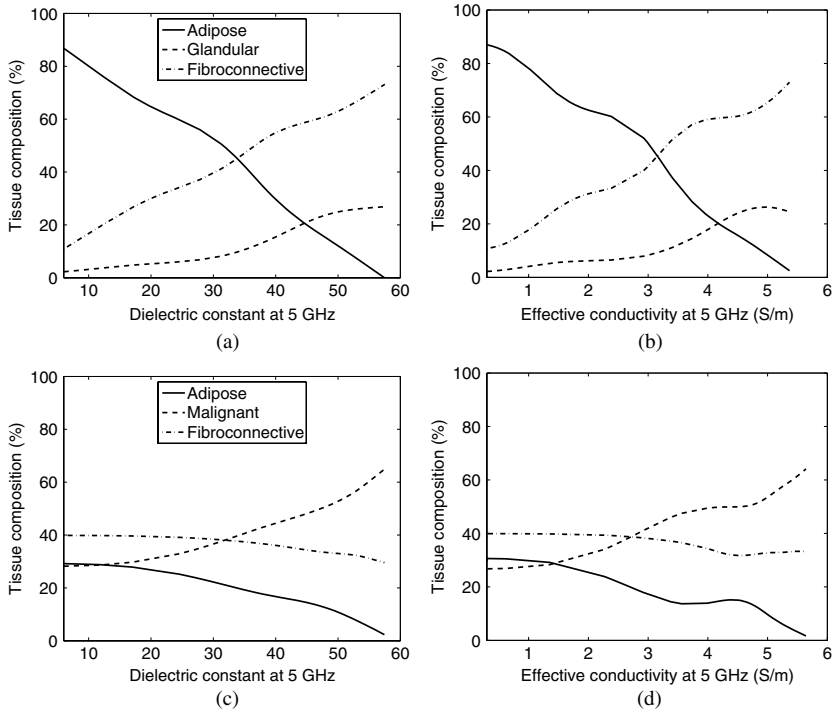

Figure 11. Per cent tissue type as a function of dielectric constant and effective conductivity at 5 GHz for (a) and (b) tissue samples diagnosed as normal and (c) and (d) tissue samples diagnosed as cancer.

Figures 11(c) and (d) illustrate that in general, as the dielectric constant and effective conductivity at 5 GHz increase, the malignant tissue content increases, while the adipose tissue content decreases. These trends are intuitive, since the low-water-content adipose tissue has low dielectric properties, while the high-water-content malignant tissue has high dielectric properties. We note that there is no curve for normal glandular tissue content in these plots because it is very difficult to generate smooth curves for a tissue type that is present in such small quantities.

4.8. Incorporating the results of this study into numerical and physical breast phantoms

The compact Cole–Cole representations of the wideband dielectric properties reported in tables 2, 3 and 4 and in Lazebnik *et al* (2007a) can serve as benchmarks in the design of numerical breast phantoms with dispersion models that are suitable for computational electromagnetics simulations of microwave imaging and cancer detection, monitoring and treatment systems. For example, in Lazebnik *et al* (2007b), we proposed highly accurate one- and two-pole Debye models for the three adipose-defined groups for normal breast tissues. The two-pole models are in excellent agreement with the benchmark Cole–Cole models over the entire 0.5–20 GHz frequency range, while the one-pole Debye models are in excellent agreement with the Cole–Cole models over the 3.1–10.6 GHz frequency range, which corresponds to the FCC-authorized band for ultrawideband medical imaging systems (Federal Communications Commission 2003).

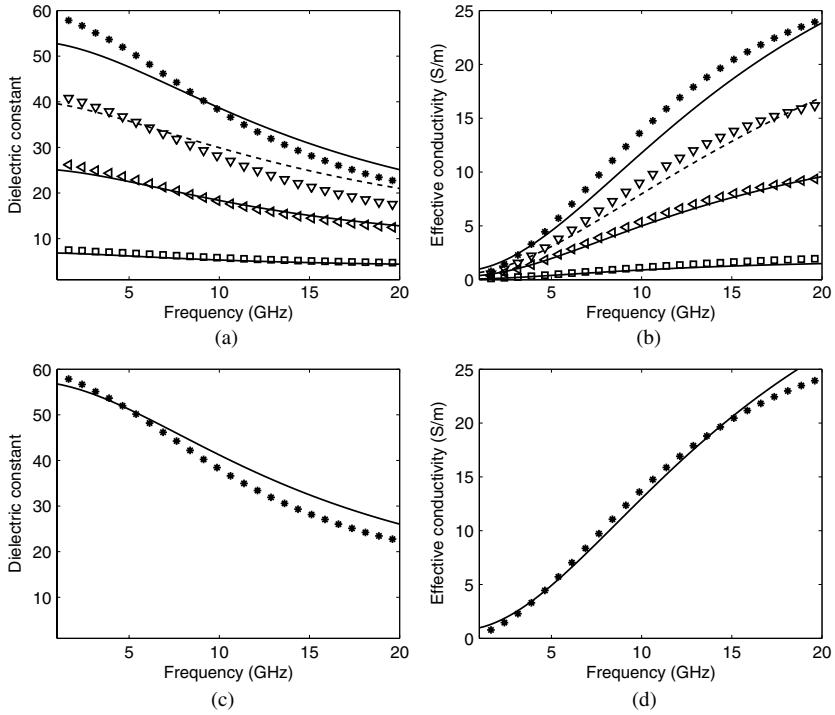

Figure 12. Comparison of our median Cole–Cole curves for normal and malignant tissue with measured dielectric properties of TM phantom materials (Lazebnik *et al* 2005). (a) and (b) Dielectric constant and effective conductivity, respectively, for the three adipose-defined normal tissue groups. Solid lines: median Cole–Cole curves for normal tissue samples obtained from cancer surgeries (in the order of highest to lowest dielectric properties: group 1, group 2 and group 3). Dashed lines: median Cole–Cole curves for group 2 for normal tissue samples obtained from reduction surgeries. (c) and (d) Median Cole–Cole curves for the dielectric constant and effective conductivity, respectively, of cancer samples with minimum malignant tissue content of 30%. Symbols: measured dielectric properties of TM phantom materials ($*$, 10% oil; $\triangledown$, 30% oil; $\triangleleft$; 50% oil; $\square$, 80% oil).

The results of this large-scale study can also serve as benchmarks in the design of materials for use in physical breast phantoms. To illustrate one possible approach, we compare the dielectric properties of previously developed tissue-mimicking (TM) phantom materials (Lazebnik *et al* 2005) to the median dielectric properties of normal and cancer tissues summarized by the Cole–Cole parameters in tables 2–4. Lazebnik *et al* (2005) previously demonstrated that the TM materials can be customized to simulate a variety of biological tissues over a wide frequency range by carefully controlling the composition of the oil-in-gelatin dispersions. Figures 12(a) and (b) show the median Cole–Cole curves of the three adipose-defined groups for normal breast tissues obtained from reduction and cancer surgeries. For groups 1 and 3, we show only the median Cole–Cole curves for normal breast tissues obtained from cancer surgeries (top solid lines: group 1, bottom solid lines: group 3), since we showed in section 4.5 that the median Cole–Cole curves for tissues obtained from cancer and reduction surgeries are very similar for these two groups. For group 2, we show the median Cole–Cole curves for normal tissues obtained from both cancer (middle solid lines) and reduction (dashed lines) surgeries. The symbols show the measured dielectric

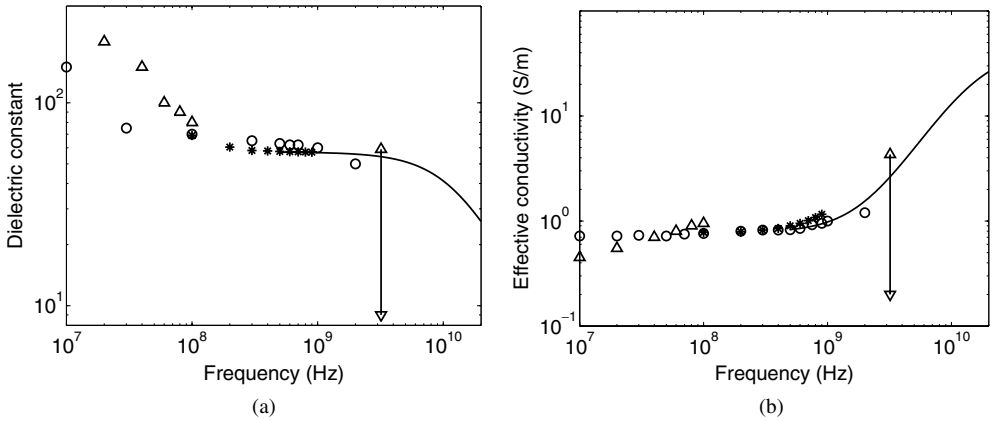

Figure 13. Comparison of our malignant tissue data with previous studies. Lines: median dielectric properties of the cancer samples from our study with 30% or greater malignant tissue content. Symbols: malignant breast tissue dielectric properties data published previously (○, Chaudhary *et al* (1984); △, Surowiec *et al* (1988); ∗, Joines *et al* (1994)). Vertical arrows: range of data reported by Campbell and Land (1992) at 3.2 GHz for malignant tissues.

properties of TM phantom materials. In the order of highest to lowest dielectric properties, the compositions of the TM materials are 10% oil, 30% oil, 50% oil and 80% oil. The dielectric properties of these four compositions of TM materials agree with the median Cole–Cole curves of normal breast tissues very well over the entire 0.5–20 GHz frequency range. Similarly, figures 12(c) and (d) show the median Cole–Cole curves for the dielectric constant and effective conductivity of cancer samples with minimum malignant tissue content of 30%. The symbols show the measured dielectric properties of TM materials with 10% oil. Again, the dielectric properties of phantom materials with this composition agree with the median Cole–Cole curves for malignant breast tissue very well from 0.5 to 20 GHz. Consequently, we recommend utilizing our TM materials containing 10–80% oil to simulate the various normal and malignant breast tissues that one might wish to include in a realistic experimental breast phantom.

4.9. Comparison with previous studies

Figure 13 shows the median curves (lines) of the cancer samples characterized in this study with 30% or more malignant tissue content, along with data points (symbols) that represent results published in three earlier studies (Chaudhary *et al* 1984, Surowiec *et al* 1988, Joines *et al* 1994) for malignant breast tissues. The data reported in this study agree extremely well with previously published results. The vertical arrows represent the range of data reported in Campbell and Land (1992) at 3.2 GHz for malignant breast tissues. The median dielectric properties for breast cancer samples reported in our study fall near the top of the range given in Campbell and Land (1992).

Some of the previously published small-scale studies reported considerable dielectric-properties contrast between normal and malignant breast tissues at microwave frequencies. For example, Chaudhary *et al* (1984), who analyzed normal and malignant breast tissue from 15 patients, found that the dielectric properties of malignant breast tissues at 1–2 GHz were approximately 300–500% greater than the dielectric properties of normal tissues at these

frequencies. Similarly, Joines *et al* (1994), who analyzed 12 measurements on normal breast tissue and 12 measurements on malignant breast tissue, found that the dielectric properties of malignant tissues were approximately 200–500% greater than the dielectric properties of normal tissues at 900 MHz. These results, combined with the results of our statistical analysis using the third technique presented earlier in this section, lead us to speculate that the normal tissues in these small-scale studies may have had significant adipose content. As a result, the contrasts reported in these studies were likely dielectric-properties contrasts between normal adipose tissue and malignant glandular tissue. In contrast, Campbell and Land (1992), who analyzed 22 normal and 41 diseased (malignant or benign) tissue samples at 3.2 GHz and distinguished between normal high-water-content tissue and adipose tissue in the breast, concluded that there was very little contrast between the dielectric properties of normal and diseased breast tissue. This conclusion is consistent with the results of our statistical analysis using the first two techniques presented in this section.

5. Summary and conclusions

In this paper, we reported the ultrawideband dielectric properties of 155 normal, cancer and benign breast tissue samples from 0.5 to 20 GHz obtained from cancer surgeries at the University of Wisconsin and University of Calgary hospitals. We fit a one-pole Cole–Cole model to the complex permittivity data set collected for each sample. We found that the dielectric properties of normal tissues span a very large range, from very low lipid-like dielectric properties to high dielectric properties approaching those of saline. This finding is consistent with our conclusions from characterizing a large number of normal tissue samples from breast reduction surgeries (Lazebnik *et al* 2007a). In contrast, we found that the dielectric properties of malignant tissues are high and span a relatively small range. We also found that the dielectric properties of benign tissues are similar to the properties of lower-adipose-content normal breast tissues.

We investigated three statistical analysis techniques of comparing the dielectric properties of cancer samples (containing 30% or more malignant tissue) with the dielectric properties of normal samples obtained from cancer surgeries. First, we adjusted for adipose tissue content of all samples by only comparing the mean dielectric properties of samples that contained 0–10% adipose content. Second, we adjusted for the content of both adipose and fibroconnective tissues in all samples. Finally, as an instructive counter-example, we did not adjust for the content of adipose or fibroconnective tissues, and compared the mean dielectric properties of all malignant samples containing 30% or greater cancer tissue with all normal samples characterized in this study. The results of our analyses indicate that the microwave-frequency dielectric-properties contrast between malignant breast tissues and normal adipose-dominated breast tissues is large, ranging up to a 10:1 contrast when considering almost entirely adipose breast tissue as the reference. In contrast, the dielectric-properties contrast between malignant and normal fibroconnective/glandular breast tissues is considerably lower, no more than approximately 10%.

In addition, we found that secondary factors, such as the time between measurement and excision, sample temperature (within the range of temperatures observed in this study), and patient age have negligible effects on the dielectric properties of breast tissues. Furthermore, there is no statistically significant difference in the within-patient and between-patient variability of the dielectric properties. The compact Cole–Cole representation for the wideband dielectric properties makes it possible to readily incorporate accurate dielectric-properties values into future numerical and experimental breast phantoms used in the development of microwave breast imaging and breast cancer detection, monitoring, and treatment applications.

Acknowledgments

The authors would like to express their gratitude to the following individuals at the University of Wisconsin and University of Calgary Hospitals for their assistance with and support of this work: Theresa Bergholz, Dr Kennedy Gilchrist, Deb Gawin, Kirk Headley, Linda Jacobs, Dr Frederick Kelcz, Dr Eberhard Mack, Dr David Mahvi, Debra Martin, Pauline Orton, Brian Shin, Dr Fushen Xu, and Jan Yakey. In addition, we would like to thank Kaitlyn Booske, Lisa Chung, Dr Mark Converse, and Dina Hagl for their assistance with several of the measurements and some of the data analysis. This work was supported by the National Institutes of Health under grant R01CA087007 awarded by the National Cancer Institute, the National Science Foundation under a Graduate Research Fellowship, the Natural Sciences and Engineering Research Council of Canada, and the Canadian Breast Cancer Foundation.

References

Alberts B, Johnson A, Lewis J, Raff M, Roberts K and Walter P 2002 *Molecular Biology of the Cell* 4th edn (New York: Garland Science) p 1325

American Cancer Society 2007 *Cancer Facts and Figures 2007* Available at www.cancer.org

Bond E J, Li X, Hagness S C and Van Veen B D 2003 Microwave imaging via space-time beamforming for early detection of breast cancer *IEEE Trans. Antennas Propagat.* **51** 1690–705

Bulyshev A E, Semenov S Y, Souvorov A E, Svenson R H, Nazarov A G, Sizov Y E and Tatsis G P 2001 Computational modeling of three-dimensional microwave tomography of breast cancer *IEEE Trans. Biomed. Eng.* **48** 1053–6

Campbell A M and Land D V 1992 Dielectric properties of female human breast tissue measured *in vitro* at 3.2 GHz *Phys. Med. Biol.* **37** 193–210

Chaudhary S S, Mishra R K, Swarup A and Thomas J M 1984 Dielectric properties of normal and malignant human breast tissues at radiowave and microwave frequencies *Indian J. Biochem. Biophys.* **21** 76–9

Chen Y F, Gunawan E, Low K S, Wang S C, Kim Y and Soh C B 2007 Pulse design for time reversal method as applied to ultrawideband microwave breast cancer detection: a two-dimensional analysis *IEEE Trans. Ant. Prop.* **55** 194–204

Conover W J 2001 *Practical Nonparameteric Statistics* 3rd edn (New York: Wiley)

Converse M, Bond E J, Van Veen B D and Hagness S C 2004 Ultrawideband microwave space-time beamforming for hyperthermia treatment of breast cancer: a computational feasibility study *IEEE Trans. Microw. Theory Tech.* **52** 1876–89

Converse M, Bond E J, Van Veen B D and Hagness S C 2006 A computational study of ultrawideband versus narrowband microwave hyperthermia for breast cancer treatment *IEEE Trans. Microw. Theory Tech.* **54** 2169–80

Davis S K, Tandradinata H, Hagness S C and Van Veen B D 2005 Ultrawideband microwave breast cancer detection: A detection-theoretic approach using the generalized likelihood ratio test *IEEE Trans. Biomed. Eng.* **52** 1237–50

El-Shenawee M 2004 Resonant spectra of malignant breast cancer tumors using the three-dimensional electromagnetic fast multipole model *IEEE Trans. Biomed. Eng.* **51** 35–44

Everitt B S and Dunn G 2000 *Applied Multivariate Data Analysis* (London: Arnold)

Fear E C, Hagness S C, Meaney P M, Okoniewski M and Stuchly M A 2002 Enhancing breast tumor detection with near-field imaging *IEEE Microw. Mag.* **3** 48–56

Fear E C, Sill J and Stuchly M A 2003 Experimental feasibility study of confocal microwave imaging for breast tumor detection *IEEE Trans. Microw. Theory Tech.* **51** 887–92

Fear E C 2005 Microwave imaging of the breast *Technol. Cancer Res. Treat.* **4** 69–82

Federal Communications Commission 2003 Available at http://www.fcc.gov/Bureaus/Engineering_Technology/News_Releases/2002/nret0203.html

Fenn A J, Wolf G L and Fogle R M 1999 An adaptive microwave phase array for targeted heating of tumours in intact breast: animal study results *Int. J. Hyperthermia* **15** 45–61

Gabriel S, Lau R W and Gabriel C 1996 The dielectric properties of biological tissues: III. Parametric models for the dielectric spectrum of tissues *Phys. Med. Biol.* **41** 2271–93

Hagness S C, Taflove A and Bridges J E 1998 Two-dimensional FDTD analysis of a pulsed microwave confocal system for breast cancer detection: fixed-focus and antenna-array sensors *IEEE Trans. Biomed. Eng.* **45** 1470–9

Hagl D M, Popovic D, Hagness S C, Booske J H and Okoniewski M 2003 Sensing volume of open-ended coaxial probes for dielectric characterization of breast tissue at microwave frequencies *IEEE Trans. Microw. Theory Tech.* **51** 1194–206

Hilland J 1997 Simple sensor system for measuring the dielectric properties of saline solutions *Meas. Sci. Technol.* **8** 901–10

Huo Y, Bansal R and Zhu Q 2004 Modeling of noninvasive microwave characterization of breast tumors *IEEE Trans. Biomed. Eng.* **51** 1089–94

Joines W T, Zhang Y, Li C and Jirtle R L 1994 The measured electrical properties of normal and malignant human tissues from 50 to 900 MHz *Med. Phys.* **21** 547–50

Kosmas P and Rappaport C M 2006 FDTD-based time reversal for microwave breast cancer detection - Localization in three dimensions *IEEE Trans. Microw. Theory Tech.* **54** 1921–7

Lazebnik M *et al* 2007a A large-scale study of the ultrawideband microwave dielectric properties of normal breast tissue obtained from reduction surgeries *Phys. Med. Biol.* **52** 2637–56

Lazebnik M, Madsen E L, Frank G R and Hagness S C 2005 Tissue-mimicking phantom materials for narrowband and ulrawideband microwave applications *Phys. Med. Biol.* **50** 4245–58

Lazebnik M, Okoniewski M, Booske J H and Hagness S C 2007b Highly accurate Debye models for normal and malignant breast tissue dielectric properties at microwave frequencies *IEEE Microw. Wireless Comp. Lett.* at press

Li X, Bond E J, Van Veen B D and Hagness S C 2005 An overview of ultrawideband microwave imaging via space-time beamforming for early-stage breast cancer detection *IEEE Antennas Propag. Mag.* **47** 19–34

Li X, Davis S K, Hagness S C, van der Weide D W and Van Veen B D 2004 Microwave imaging via space-time beamforming: experimental investigation of tumor detection in multi-layer breast phantoms *IEEE Trans. Microw. Theory Tech.* **52** 1856–65

Meaney P M, Fanning M W, Li D, Poplack S P and Paulsen K D 2000 A clinical prototype for active microwave imaging of the breast *IEEE Trans. Microw. Theory Tech.* **48** 1841–53

Meaney P M, Fanning M W, Raynolds T, Fox C J, Fang Q Q, Kogel C A, Poplack S P and Paulsen K D 2007 Initial clinical experience with microwave breast imaging in women with normal mammography *Acad. Radiol.* **14** 207–18

Popovic D, McCartney L, Beasley C, Lazebnik M, Okoniewski M, Hagness S C and Booske J 2005 Precision open-ended coaxial probes for *in vivo* and *ex vivo* dielectric spectroscopy of biological tissues at microwave frequencies *IEEE Trans. Microw. Theory Tech.* **53** 1713–22

Sha L, Ward E R and Stroy B 2002 A review of dielectric properties of normal and malignant breast tissue *Proc. IEEE SoutheastCon* pp 457–62

Surowiec A J, Stuchly S S, Barr J R and Swarup A 1988 Dielectric properties of breast carcinoma and the surrounding tissues *IEEE Trans. Biomed. Eng.* **35** 257–63

Vargas H I, Dooley W C, Gardner R A, Gonzalez K D, Venegas R, Heywang-Kobrunner S H and Fenn A J 2004 Focused microwave phased array thermotherapy for ablation of early-stage breast cancer: results of thermal dose escalation *Ann. Surg. Oncol.* **11** 139–46

Winters D W, Bond E J, Van Veen B D and Hagness S C Estimation of the frequency-dependent average dielectric properties of breast tissue using a time-domain inverse scattering technique *IEEE Trans. Antennas Prop.* **54** 3517–28

Xie Y, Guo B, Xu L Z, Li J and Stoica P 2006 Multistatic adaptive microwave imaging for early breast cancer detection *IEEE Trans. Biomed. Eng.* **53** 1647–57

Zastrow E, Davis S K and Hagness S C 2007 Safety assessment of breast cancer detection via ultrawideband microwave radar operating in pulsed-radiation mode *Microw. Opt. Technol. Lett.* **49** 221–5

Zhang Z Q, Liu Q, Xiao C, Ward E, Ybarra G and Joines W T 2003 Microwave breast imaging: 3D forward scattering simulation *IEEE Trans. Biomed. Eng.* **50** 1180–9